Mutation of a Single TMVI Residue, Phe^{282}, in the β_2-Adrenergic Receptor Results in Structurally Distinct Activated Receptor Conformations†

Songhai Chen,‡,§ Fang Lin,‡,§ Ming Xu,‡ R. Peter Riek,‡ Jiri Novotny,‡ and Robert M. Graham*,‡,||

Molecular Cardiology and Biocomputing Units, Victor Chang Cardiac Research Institute, St. Vincent's Hospital, Darlinghurst, NSW 2010, and Faculty of Medicine and School of Biochemistry and Molecular Genetics, University of New South Wales, Kensington, NSW 2033, Australia

Received December 21, 2001; Revised Manuscript Received March 5, 2002

ABSTRACT: We showed previously that Phe^{303} in transmembrane segment (TM) VI of the α_{1B}-adrenergic receptor (α_{1B}-AR), a residue conserved in many G protein-coupled receptors (GPCRs), is critically involved in coupling agonist binding with TM helical movement and G protein activation. Here the equivalent residue, Phe^{282}, in the β_2-AR was evaluated by mutation to glycine, asparagine, alanine, or leucine. Except for F282N, which exhibits attenuated basal and maximal isoproterenol stimulation, the Phe^{282} mutants display varying degrees of constitutive activity (F282L > F282A > F282G), and as shown by the results of substituted cysteine accessibility method (SCAM) studies, induce movement of endogenous cysteine-(s) into the water-accessible ligand-binding pocket. For F282A, movement is confined to Cys^{285} in TMVI, whereas F282L induces movement of both Cys^{285} in TMVI and Cys^{327} in TMVII. Further, engineered *cysteine-sensor* studies indicate that F282L causes movement of TMVI, both above and below an apparent kink-inducing TMVI proline (Pro^{288}), whereas that due to F282A is confined to the domain below Pro^{288}. A plausible interpretation of these data is that receptor activation involves rigid body movement of TMVI which, because of its Pro^{288}-induced kink, acts as a pivot to transduce and amplify the agonist-induced conformational change in the upper domain, to a change in the lower domain required for productive receptor−G protein coupling.

G protein-coupled receptors (GPCRs) are a superfamily of more than 1000 distinct proteins. They recognize ligands as diverse as light, odorants, Ca^{2+}, proteins, and small molecules, including amino acids, nucleotides, and peptides (*1*). Although ligand−receptor interactions have been studied in detail for many GPCRs, the mechanisms whereby ligand binding leads to activation are not well-understood. Recent studies of rhodopsin (*2*), the α_{1B}-AR (*3*), the β_2-AR (*4*), and muscarinic (*5*), thyroid-stimulating hormone (TSH) (*6*), and C5a (*7*) receptors suggest that conformational changes of transmembrane helices (TMs) are involved in receptor activation. In particular, these studies indicate that receptor activation involves critical conformational changes in TMIII and TMVI. Although activation generally requires initial binding of ligand, activation of receptor-coupled intracellular second messengers can also be observed in some circumstances in the absence of agonist. This phenomenon, termed constitutive activity, is observed with point mutations of residues located in virtually all different receptor domains, that is, the extra- and intracellular regions and TM helices (*8*, *9*). On the basis of the prevailing two-state model for GPCR activation, whereby the receptor exists in equilibrium between an inactive state, R, and an active state, R*, constitutive activity has been interpreted to result from mutation-induced shifts in this equilibrium. This, in turn, leads to a higher proportion of receptor molecules in the active state, R* (*8*). Studies of rhodopsin (*10*) and the α_{1B}-AR (*11*, *12*) suggest that constitutively active mutants can arise from disruption of a salt bridge between TMIII and TMVII. In addition, charge-neutralizing mutants of Asp or Glu in the conserved E/DRY motif of GPCRs can also constitutively activate receptors (*13*−*16*). Interestingly, various constitutively active β_2-AR mutants that result from point mutations of residues at several different receptor locations, e.g., substitutions in the DRY motif at the end of TMIII (*16*), or of residues at the C-terminal end of the third intracellular loop (*17*), are associated with movement of TMVI, a conformational change also observed with agonist-mediated receptor activation. This argues strongly that mutants producing constitutive activity do so by inducing conformational changes similar to those resulting from agonist activation.

We showed previously that various substitutions of Phe^{303} in TMVI of the α_{1B}-AR, a highly conserved residue in GPCRs, result in receptor mutants with different functional activity (*3*). Subsequent thermal stability and SCAM studies of Phe^{303} to Gly, Asn, Ala, and Leu substitution mutants indicated that they induce distinct TM helical movements (*18*). Further identification of the TM helices involved in the conformational changes induced by the Phe^{303} substitu-

† Supported by grants from the National Health and Medical Research Council, Australia.

* To whom correspondence should be addressed: Victor Chang Cardiac Research Institute, 384 Victoria St., Darlinghurst, Sydney, NSW 2010, Australia. E-mail: b.graham@victorchang.unsw.edu.au.

‡ St. Vincent's Hospital.

§ Present address: Department of Pharmacology, Vanderbilt University Medical Center, 444 Robinson Research Building, Nashville, TN 37232. E-mail: songhai.chen@mcmail.vanderbilt.edu and fang.lin@mcmail.vanderbilt.edu.

|| University of New South Wales.

10.1021/bi012189c CCC: $22.00
Published on Web 04/17/2002

tions, however, was hampered by the fact that the wild-type α_{1B}-AR is sensitive to methanethiosulfonate ethylammonium (MTSEA) derivatization due to an endogenous membrane-embedded cysteine, Cys[129], that faces the ligand-binding pocket. This necessitated initial development of an MTSEA-insensitive C129S mutant as a template for subsequent analysis. The requirement of this additional mutation limited expression and evaluation of subsequent triple or quadruple mutants, incorporating the Phe[303] substitutions, as well as mutations aimed at clarifying which additional endogenous TM-embedded cysteine(s) had moved into the water-accessible ligand-binding pocket (*18*). In contrast to the α_{1B}-AR, the wild-type β_2-AR is MTSEA-insensitive as it lacks a cysteine at the position equivalent to position 129 (*16*, *17*). Since the β_2-AR does not require initial substitution of a Cys[129] homologue, we reasoned that it would be a useful template for defining, in detail, the TM helical movements associated with constitutively active mutants. Further, as the α_{1B}-AR Phe[303] equivalent is highly conserved in GPCRs and mutation of this residue alters the functional activity of many receptors, we questioned here if the Phe[303] equivalent in the β_2-AR, a GPCR whose sequence is homologous to a limited degree (36%) to that of the α_{1B}-AR, has similar critical structural and functional properties. Thus, in this study, we constructed and evaluated Gly, Asn, Ala, or Leu substitutions of Phe[282] in the β_2-AR (Figure 1). Like the Phe[303] α_{1B}-AR mutants, the corresponding Phe[282] mutants displayed altered signaling activity and different TM helical movements. In particular, using SCAM studies, we show that the TM movement associated with F282A was confined to the lower segment of TMVI. On the other hand, F282L, a mutation resulting in marked constitutive activity, induced movements of both the upper and lower segments of TMVI about a highly conserved proline, Pro[288], that likely induces a kink in this TM helix. Taken together, these findings indicate that a critical role of the TMVI Phe (Phe[282]) in coupling movements of this helix to G protein activation is likely to be a conserved feature of many GPCRs.

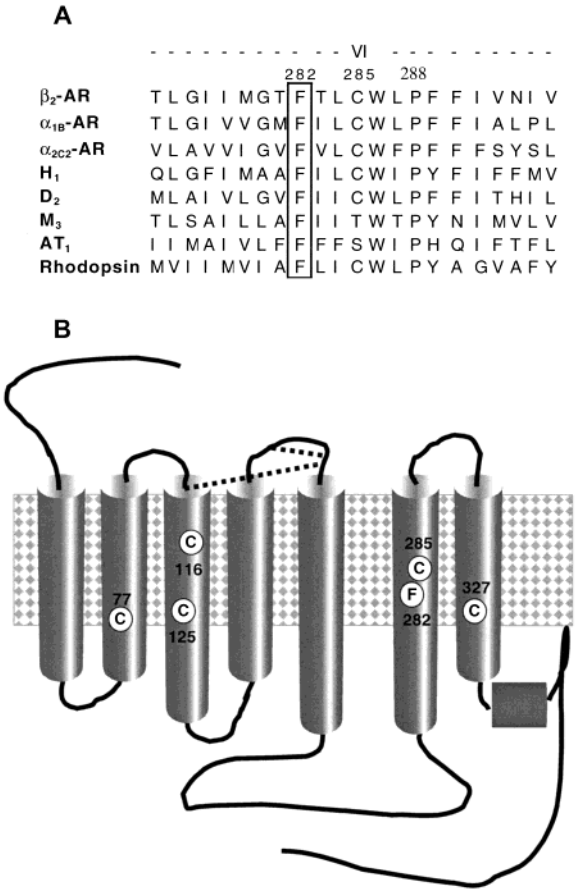

FIGURE 1: Sequence alignment of TMVI residues of hamster β_2 and other G protein-coupled receptors and topographical model of the hamster β_2-AR. (A) Sequences were aligned to maximize homology within this region using the GCG program "Pileup". The conserved phenylalanines, corresponding to F282 of the β_2-AR, are boxed. The dashed line at the top delineates the transmembrane residues of helix VI. (B) Topographical model of the hamster β_2-AR indicating the location of the native membrane-embedded cysteine residues, as well as the location of two disulfide bonds (dashed lines) linking the extracellular pairs, Cys[106] and Cys[191], and Cys[184] and Cys[190], and residue Phe[282] evaluated in this study.

EXPERIMENTAL PROCEDURES

Materials. (−)-Isoproterenol and DL-propranolol were purchased from Sigma. GMP-PNP was from Roche Molecular Biochemicals. Pindolol, (±)-CGP12177, and ICI118, 551[1] were from Research Biochemicals International. Fetal calf serum and culture media were from Life Technologies. Cyclic AMP assay kits were from Amersham, and [^{125}I]iodocyanopindolol ([^{125}I]CYP, 2200 Ci/mmol) and [^{3}H]CGP12177 (40 Ci/mmol) were from NEN Life Science. Methanethiosulfonate ethylammonium was from Toronto Research Chemicals Inc. The QuikChange site-directed mutagenesis kit was from Stratagene. Other chemicals were of the highest grade available commercially.

Mutagenesis. β_2-AR mutants were generated using the QuikChange site-directed mutagenesis kit (Stratagene) using a total synthetic hamster β_2-AR gene in the mammalian expression vector, pMT2′ (*19*). Briefly, two synthetic oligonucleotide primers, each complementary to opposite strands of the vector and containing the desired mutation, were annealed to pMT2′β_2-AR and extended by PCR using *Pfu* DNA polymerase. The amplified product, after digestion with *Dpn*I to remove the parental DNA template, was then transformed into DH5α′ cells. Plasmid DNA was prepared from the resultant colonies and sequenced to confirm the presence of the desired mutation.

Cell Culture and Transfection. COS-1 cells (American Type Culture Collection, Rockville, MD) were cultured and transiently transfected with the indicated constructs using the DEAE-dextran method, as described previously (*3*, *20*), except that for cAMP measurement, cells were plated in 12-well plates and transfected with 2−40 ng of wild-type or 0.02−2.5 μg of mutant pMT2′β_2-ARs using 2 μL of LipofectAMINE 2000 (Life Technologies) in 0.5 mL of Opti-MEM (Life Technologies) per well. Cells were harvested 72 h post-transfection.

Membrane Preparation. Membranes were prepared from transfected COS-1 cells, as described previously (*3*, *20*). The membranes were resuspended in TEM buffer [10 mM Tris-

[1] Abbreviations: [^{3}H]CGP12177, [^{3}H]-4-{3-[(1,1-dimethylethyl)-amino]-2-hydroxypropoxy}-1,3-dihydro-2*H*-benzimidazole-2; ICI118, 551, (±)-1-[2,3-(dihydro-7-methyl-1*H*-inden-4-yl)oxy]-3-[(1-methylethyl)-amino]-2-butanol; DEAE, diethylaminoethyl; EC_{50}, concentration of agonist required to produce 50% of the maximal response; E_{max}, maximal effector response.

Table 1: Ligand Binding Profiles of Wild-Type and Phe^{282} Mutant β_2-ARs[a]

	[(−)-isoproterenol] (nM)					
	without GMP-PNP					
construct	$K_{i,high}$	$K_{i,low}$	with GMP-PNP	[pindolol] (nM)	[(±)-CGP12177] (nM)	[[^{125}I]CYP] (pM)
wild type		111 ± 18	177 ± 39	2.98 ± 0.96	2.04 ± 0.49	123 ± 16
F282G	1.2 ± 0.3 (0.35 ± 0.13)	12.9 ± 1.2 [8.6]	18.2 ± 4.4	1.67 ± 0.45	2.47 ± 0.8	56 ± 1
F282N		42 ± 9.2 [2.6]	61.7 ± 16.9	2.1 ± 0.44	1.8 ± 0.58	85 ± 22
F282A	2.1 ± 0.15 (0.77 ± 0.05)	32.3 ± 6.7 [3.4]	31.7 ± 7.6	1.18 ± 0.45	3.23 ± 1.75	147 ± 56
F282L	0.71 ± 0.08* (0.73 ± 0.03)	18.4 ± 2.8* [6.0]	20.5 ± 6.3*	1.58 ± 0.56	3.8 ± 1.94	77 ± 9

[a] Using membranes prepared from transfected COS-1 cells, the binding affinities (K_i) of (−)-isoproterenol, in the presence and absence of GMP-PNP (100 μM), as well as pindolol and (±)-CGP12177 were determined from [^{125}I]CYP competition binding studies. The affinity of [^{125}I]CYP (K_D) was determined by saturation binding as described in Experimental Procedures. Data are presented as means ± one standard error of at least three independent experiments, each performed in duplicate. Values in parentheses and brackets are the fraction of high-affinity binding sites and the ratio of the wild-type to mutant β_2-AR $K_{i,low}$ values, respectively. Asterisks indicate a difference ($p < 0.01$) vs the respective F282A values.

HCl (pH 7.5), 1.5 mM EGTA, and 12.5 mM $MgCl_2$] containing 10% (v/v) glycerol and stored at −70 °C. Protein concentrations were determined by the Bradford method (*21*).

Ligand Binding. The ligand binding characteristics of the membrane-expressed receptors were determined in a series of radioligand binding studies performed exactly as described previously (*3*, *20*), using [^{125}I]CYP, a β-AR antagonist, as the radioligand. Binding data were analyzed using the iterative, nonlinear, curve-fitting program Prism.

Cyclic AMP Generation. Forty-eight hours after transfection, the growth medium for COS-1 cells was replaced with 1 mL of DMEM containing 1% dialyzed FCS, and the cells were incubated for an additional 24 h. β_2-AR-mediated cAMP accumulation was then assessed as described previously (*3*). Briefly, cells were first incubated in serum-free medium for 2−3 h and then preincubated with 3-isobutyl-1-methylxanthine (250 μM) for 20 min before the addition of agonists. The reaction was terminated after 20 min by addition of ice-cold cell lysis buffer. After disruption of cells by sonication, cAMP levels in the crude cell lysate were determined using the [^{125}I]cAMP scintillation proximity assay (SPA) system (Amersham) for nonacetylated cAMP according to the manufacturer's instructions.

MTSEA Derivatization and Binding Assays in Intact Cells. Reaction of transfected COS-1 cells with MTSEA was performed at room temperature for 2 min as described previously (*20*), except that for double and triple mutants, which were expressed at lower levels, the reaction volume was increased to 0.5 mL to allow more cells to be used. Cell suspensions were then diluted 10−20-fold and used to assay for [^{3}H]CGP12177 (4 nM) or [^{125}I]CYP (2 nM) binding in the presence or absence of 0.1 mM DL-propranolol. To exclude the influence of the endogenously expressed β_2-AR in COS-1 cells, cells transfected with pMT2′ alone were always included in the studies and the binding results were subtracted from the above data.

Computer-Aided Modeling of the β_2-AR. A three-dimensional model of the seven TM helices of the β_2-AR was constructed using the program ICM (Molsoft Inc., La Jolla, CA), with the X-ray crystallographic structure of bovine rhodopsin (*22*) serving as the template. Briefly, amino acid sequences of the β_2-AR and bovine opsin were aligned, yielding 22% identical residues in the seven transmembrane segments. On the basis of the alignment, seven distinct peptides corresponding to the β_2-AR TM helices were constructed using ICM. These were tethered by harmonic constraints to their corresponding opsin TM helices and assembled into helical conformations by successive manipulations of selected degrees of freedom (rigid body rotational/translational, then torsional). Once assembled, the TM segments were extensively minimized with respect to their full atomic, molecular mechanics potential. When the resulting β_2-AR model was superimposed on the rhodopsin X-ray structure, it differed, in terms of the 772 backbone atoms modeled, by an rmsd of only 1.1 Å.

Residue Numbering. The residue numbers are those for the hamster β_2- and α_{1B}-ARs. For comparison with the Ballestros−Weinstein numbering scheme (*23*), β_2-AR residues Phe^{282}, Cys^{285}, Pro^{288}, and Cys^{327} are Phe$^{6.44}$, Cys$^{6.47}$, Pro$^{6.50}$, and Cys$^{7.54}$, respectively.

Data Analysis. Results are expressed as the mean ± one standard error (shown as error bars in the figures). Analysis of variance and a Student's *t* test were used to determine significant differences ($p < 0.05$) using SigmaStat software.

RESULTS

Phe^{282} in TMVI of the β_2-AR was mutated to Gly, Asp, Ala, or Leu. As shown in Table 1, all mutants exhibited little change in affinity for the antagonist radioligand, [^{125}I]CYP, the antagonist, CGP12177, or the weak partial agonist, pindolol. Their expression level was 2−10-fold lower than that of the wild-type receptor (data not shown). Competition studies with (−)-isoproterenol revealed a single class of binding sites for the wild-type receptor (K_i = 111 nM) in transfected COS-1 membranes, which was not altered by pretreatment with GMP-PNP. In contrast, (−)-isoproterenol competition curves for all mutants except F282N were best fit to a two-site model (Table 1). The K_i value for the high-affinity site ($K_{i,high}$) ranged from 0.71 to 2.1 nM and accounted for 35−77% (F282L ≈ F282A > F282G) of the total binding sites, whereas the $K_{i,low}$ equaled 13−32 nM. The high-affinity component of (−)-isoproterenol binding was abolished by pretreatment of the COS-1 membranes with GMP-PNP, residual binding being monophasic and having a K_i value identical to that of the low-affinity component ($K_{i,low}$). However, in the presence of GMP-PNP, the affinity of all Phe^{282} mutants for (−)-isoproterenol was still significantly higher than that of the wild type (3−9-fold), indicating that their high agonist affinity was not due merely to an increased level of G protein coupling, but also involved a component resulting from an intrinsic alteration in their agonist binding pocket.

The ability of the wild-type β_2-AR or Phe^{282} mutants to stimulate cAMP accumulation was examined in intact COS-1

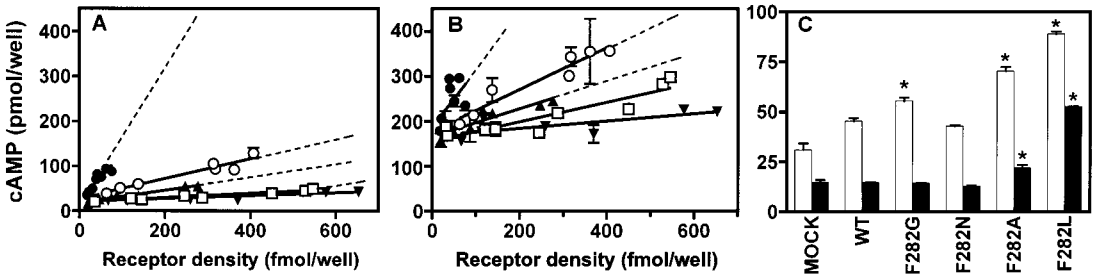

FIGURE 2: Basal and (−)-isoproterenol-stimulated cAMP accumulation. Basal (A) and 0.1 mM (−)-isoproterenol-stimulated (B) cAMP accumulation, in the presence of 3-isobutyl-1-methylxanthine (0.25 mM), was assessed over 20 min in COS-1 cells transiently expressing the wild-type β_2-AR (□), F282G (▲), F282N (▼), F282A (○), or F282L (●), as described in Experimental Procedures. (C) COS-1 cells transfected with plasmid DNA encoding vector alone (mock) or wild-type (WT) or mutant β_2-ARs were incubated in the presence (black bars) or absence (white bars) of ICI118,551 (0.1 mM) for 24 h, and then basal cAMP accumulation was assessed as described above. The cells expressed 57 fmol/mg of native β_2-AR (mock) and 608, 276, 653, 138, and 98 fmol/mg of the wild-type, F282G, F282N, F282A, and F282L mutant β_2-AR, respectively. Levels of basal and (−)-isoproterenol-stimulated cAMP accumulation were 22 ± 3 and 150 ± 15 pmol/well, respectively, in mock-transfected COS-1 cells. Asterisks indicate significant differences ($p < 0.05$) vs the corresponding level of cAMP accumulation mediated by the wild-type receptor.

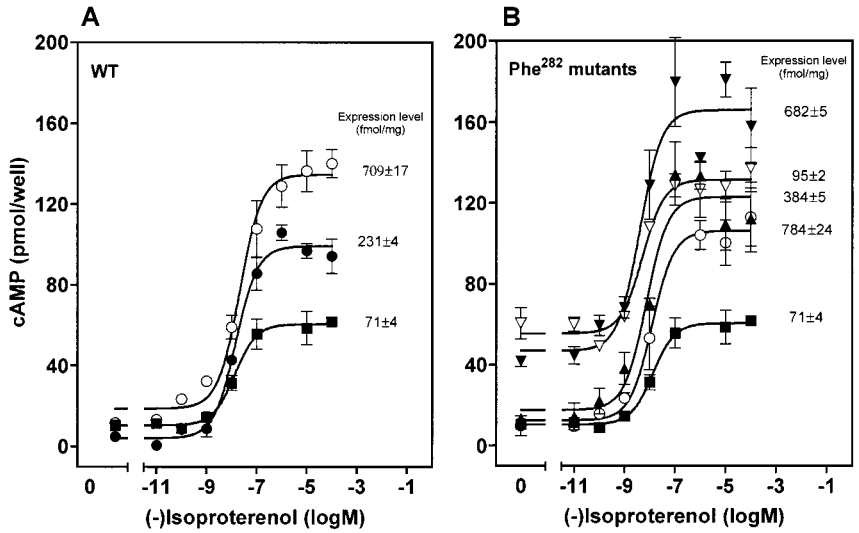

FIGURE 3: Dose-related increases in the level of cAMP accumulation with (−)-isoproterenol stimulation of wild-type and mutant β_2-ARs. The level of cAMP accumulation in intact COS-1 cells transfected with vector alone (■) or plasmid DNA encoding the wild-type β_2-AR (WT) [2 ng (●) or 25 ng (○)] (A) or Phe^{282} mutants F282A [0.5 μg, expression level = 682 ± 5 fmol/mg (▼)], F282L [2.5 μg, 95 ± 2 fmol/mg (▽)], F282G [2.5 μg, 384 ± 5 fmol/mg (▲)], and F282N [0.5 μg, 784 ± 24 fmol/mg (○)] (B) and stimulated with (−)-isoproterenol at the indicated concentrations for 20 min were determined as described in Experimental Procedures.

cells. As shown in Figure 2A, the level of basal cAMP accumulation increased linearly with an increasing level of receptor expression for the wild-type receptor and mutants, although the slope of this relationship was significantly greater ($p < 0.05$ in each case) for the F282G, F282A, and F282L mutants (0.14 ± 0.016, 0.22 ± 0.029, and 1.01 ± 0.19, respectively) but slightly lower for the F282N mutant (0.03 ± 0.009) than for the wild-type receptor (0.047 ± 0.005). The increased basal activity of the wild-type receptor and F282G mutant was eliminated by preincubation with the inverse agonist, ICI118,551, but under the same conditions, ICI118,551 only partially inhibited the basal activity of the F282A and F282L mutants (Figure 2C). Stimulation of the receptor with a saturation concentration of (−)-isoproterenol (0.1 mM) resulted in cAMP accumulation, the level of which increased linearly in relation to the level of receptor expression (Figure 2B). As observed for basal activity, the slope of this relationship was greater for the F282L (1.27 ± 0.07), F282A (0.46 ± 0.06), and F282G (0.31 ± 0.05) mutants than for the wild-type β_2-AR (0.22 ± 0.04), whereas that for the F282N (0.08 ± 0.04) mutant was lower than that for the wild-type receptor ($p < 0.05$).

We next evaluated dose−response relationships for (−)-isoproterenol-stimulated cAMP accumulation. To allow for differences in receptor expression levels, cAMP accumulation was assessed at two different levels of wild-type receptor expression. As shown in Figure 3A, activation of the wild-type receptor resulted in a dose-dependent increase in the level of cAMP accumulation, which was related to the level of receptor expression. As expected, basal activity and (−)-isoproterenol efficacy (E_{max}) increased at the higher level of receptor expression. However, consistent with a lack of spare receptors in this assay system, (−)-isoproterenol potency (EC_{50} = 21 ± 11, 49 ± 19, and 26 ± 8 nM) was not significantly altered with overexpression of the β_2-AR at either 231 or 709 fmol/mg of protein, as compared to the endogenously expressed COS-1 cell β_2-AR (71 fmol/mg of protein). Compared to the wild-type receptor, the F282N, F282G, F282A, and F282L mutants exhibited 3−10-fold increases in (−)-isoproterenol potency (EC_{50} = 13 ± 5, 6.7

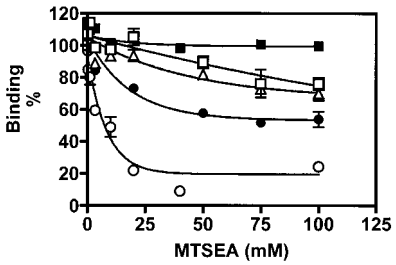

FIGURE 4: Effect of MTSEA on [^{3}H]CGP12177 binding to wild-type and mutant β_2-ARs. COS-1 cells transfected with plasmid DNA encoding the wild-type β_2-AR (■) or mutants F282G (□), F282N (△), F282A (●), and F282L (○) were incubated with the indicated concentrations of MTSEA for 2 min. Specific [^{3}H]CGP12177 binding to intact cells was then assessed as described in detail in Experimental Procedures.

$\pm$ 2.6, 3.1 $\pm$ 1.6, and 3.2 $\pm$ 1.6 nM at expression levels of 784 $\pm$ 24, 384 $\pm$ 5, 682 $\pm$ 32, and 95 $\pm$ 2 fmol/mg of protein, respectively) (Figure 3B). Basal activity and maximal cAMP accumulation for the mutants were consistent with the responses shown in Figure 2. Taken together and if one allows for differences in the levels of receptor expression, these data indicate that as compared to the wild-type receptor, the mutants exhibited constitutive activity with the following rank order of potency: F282L > F282A > F282G. On the other hand, the activity of the F282N mutant was impaired.

Possible conformational rearrangements induced by the Phe^{282} mutations were investigated using SCAM studies. As reported previously (*16*, *17*), and as illustrated in Figure 4, the wild-type β_2-AR lacks water-accessible endogenous cysteine residues. Thus, binding of [^{3}H]CGP12177 to the wild-type β_2-AR was not affected by MTSEA treatment, at concentrations up to 100 mM. In contrast, the F282G, F282N, F282A, and F282L mutants exhibited varying degrees of MTSEA sensitivity (F282L > F282A > F282G = F282N), and their inactivation by MTSEA was both dose (Figure 4)- and time-dependent (data not shown). Inhibition of radioligand binding by MTSEA was most marked for F282L (up to 80%), followed by F282A (40%) and F282G and F282N (20%). These results indicate that the constitutive activity of the F282L and F282A mutants is associated with a conformational change that renders a native cysteine(s) accessible to MTSEA derivatization.

To assess which cysteine(s) residue is responsible, we mutated the native membrane-embedded cysteines, one at a time or in combination. Valine substitution of Cys^{77}, Cys^{116}, or Cys^{125} in the F282L mutant did not significantly alter its MTSEA sensitivity (Figure 5A). In contrast, mutation of TMVI Cys^{285} to alanine, to give the double mutant F282L/C285A, resulted in a marked reduction in MTSEA sensitivity from 80 to 25% ($p < 0.05$), whereas the double mutant F282L/C327A, in which TMVII Cys^{327} was mutated, exhibited a reduction from 80 to 60% ($p < 0.05$) (Figure 5B). With the triple mutant F282L/C285A/C327A, MTSEA sensitivity was further decreased toward that observed with the wild-type receptor (Figure 5C). This indicates that the reduced MTSEA sensitivity observed when the C285A or C327A mutation was combined with the F282L mutation is directly attributable to the reduced susceptibility of these cysteines to MTSEA derivatization, and not to the alanine substitution indirectly influencing the receptor conformation and thus the accessibility of some other native cysteine (e.g., Cys^{77}, Cys^{116}, or Cys^{125}). For the F282A mutant, MTSEA sensitivity was completely abolished by substitution of alanine for Cys^{285}, but was unaltered by mutation of Cys^{327} to alanine (Figure 6). Importantly, as compared to the single mutants, F282A and F282L, neither binding of the antagonists, CGP12177 or [^{125}I]CYP, nor binding of the agonist, (−)-isoproterenol, was significantly altered by the additional cysteine mutation(s), except for the triple mutant F282L/C285A/C327A (Table 2). This mutant exhibited a slight decrease in the fraction of the high-affinity binding sites. This change is most likely due to background binding by the endogenous COS-1 cell β_2-AR, since the level of expression of the triple mutant was only 1−2-fold above that of the endogenous receptor (data not shown). Taken together, the results of these SCAM studies indicate that Cys^{285} in TMVI is solely responsible for the sensitivity of F282A to MTSEA, whereas the sensitivity of F282L involves not only Cys^{285} in TMVI but also Cys^{327} in TMVII.

We next investigated the nature of F282A- and F282L-induced movements of TMVI. As shown, alanine or leucine substitution of Phe^{282}, a residue located at the cytoplasmic end of TMVI, induces both constitutive activity and movement of this helix (evidenced by the reduced MTSEA sensitivity of the double mutants F282L/C285A and F282A/C285A, as compared to the single mutants). Thus, the conformational changes produced by the F282L and F282A mutants must, in part, involve movement of the lower segment of TMVI, a region contiguous with the receptor's G protein-interacting third intracellular loop. In addition, the finding that the residual MTSEA sensitivity that remains when C327A is combined with F282L to produce the double mutant F282L/C327A is identical to that of the F282A mutation (Figure 7A) suggests that both the Phe^{282} to alanine and leucine substitutions produce similar movements of the lower segment of TMVI.

To evaluate if F282A and F282L also induce movement of the upper segment of TMVI, Phe^{290}, a TMVI residue involved in catechol ring aromatic bonding (*24*), was substituted with a cysteine, for use as a conformational sensor. Consistent with this residue's involvement in ligand binding, and in contrast to the wild-type receptor, the F290C mutant exhibited significant inhibition of both [^{3}H]CGP12177 (data not shown) and [^{125}I]CYP binding following MTSEA treatment (Figure 7B). Since combining F290C with either the F282A/C285A or F282L/C285A/C327A mutation to generate either triple or quadruple mutants decreased the level of expression to levels that cannot be easily assessed by [^{3}H]CGP12177 binding (data not shown), the double mutants F282A/F290C and F282L/F290C were constructed and their sensitivity to MTSEA was evaluated using the high-specific activity radioligand, [^{125}I]CYP. These studies were feasible, since F290C is much more sensitive to MTSEA inactivation than F282A or F282L. Thus, the concentration of MTSEA required for maximal inactivation of F290C binding of [^{125}I]-CYP (Figure 7B) or [^{3}H]CGP12177 (data not shown) (1 mM for both radioligands) is much lower than that for inactivation of F282A or F282L binding of [^{3}H]CGP12177 (100 or 40 mM, respectively) (Figure 4). Accordingly, an effect of MTSEA on radioligand binding due to derivatization of Cys^{285} and/or Cys^{327}, which are sensitive only to high concentrations of MTSEA in the F282L and F282A structures, can be ignored when evaluating the double mutants

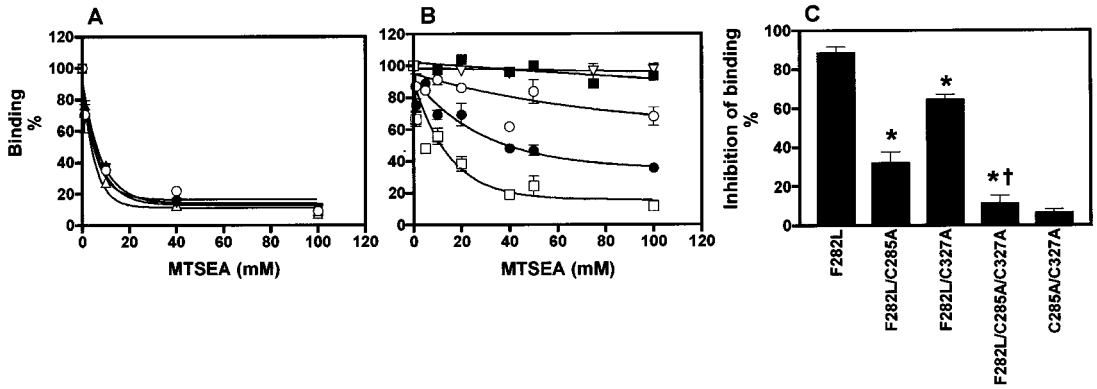

FIGURE 5: Effect of MTSEA on [^{3}H]CGP12177 binding to F282L and F282L combined with cysteine mutations. COS-1 cells transiently expressing (A) F282L (○), F282L/C77V (▲), F282L/C116V (▼), or F282L/C125V (△), (B) F282L (□), F282L/C327A (●), F282L/C285A (○), C285A (■), or C327A (▽), or (C) the mutants shown. The indicated constructs were evaluated for specific [^{3}H]CGP12177 binding, before and after treatment with MTSEA at the indicated concentrations (A and B) or 100 mM MTSEA (C) for 2 min. Specific [^{3}H]CGP12177 binding was assessed as described in the legend of Figure 4. Asterisks and daggers indicate significant differences ($p < 0.05$) vs inhibition of binding for the F282L single and double mutants, respectively.

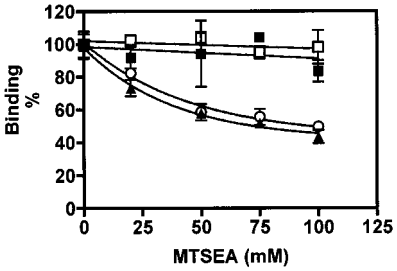

FIGURE 6: Effect of MTSEA on [^{3}H]CGP12177 binding to F282A, F282A/C285A, and F282A/C327A. MTSEA-mediated inhibition of [^{3}H]CGP12177 binding to COS-1 cells expressing F282A (▲), F282A/C285A (□), F282A/C327A (○) or C285A (■) was assessed as described in detail in Figure 4.

F290C/F282L and F290C/F282A with MTSEA concentrations of only 0.01−1 mM (Figure 7B). Moreover, interestingly, in contrast to [^{3}H]CGP12177, MTSEA did not inhibit [^{125}I]CYP binding by either F282A or F282L (Figure 7B).

The F290C, F290C/F282L, and F290C/F282A mutants bound [^{125}I]CYP with similar affinities (K_D = 202 ± 61, 185 ± 41, and 191 ± 55 pM, respectively) and, in competition studies with (−)-isoproterenol, showed only a single class of binding sites. Consistent with the Phe^{295} side chain forming an important interaction with the agonist, the affinity of the F290C mutant for (−)-isoproterenol was markedly impaired (K_i = 8.2 ± 1.3 μM). However, like the F282L and -A single mutants, the affinity of the F290C/F282L (K_i = 115 ± 18 nM) and F290C/F282A (K_i = 248 ± 45 nM) double mutants was increased by 71- and 33-fold, respectively, over that of F290C. Sensitivity of F290C (IC_{50} = 28 ± 8 μM) to MTSEA was not altered by combining F290C with F282A (IC_{50} for F282A/F290C = 36 ± 7 μM) (Figure 7B). In contrast, the MTSEA sensitivity of the F282L/F290C double mutant was significantly decreased (IC_{50} = 302 ± 28 μM, $p < 0.05$) (Figure 7B).

DISCUSSION

In this paper, we confirm and extend observations made with mutation of a Phe that is located at the intracellular end of TMVI, and that is highly conserved in many GPCRs. Like the α_{1B}-AR Phe^{303} mutants (*18*), substitution of the residue equivalent to Phe^{303} in the β_2-AR (Phe^{282}) resulted in mutants with altered signaling activity. The Gly, Ala, and Leu substitutions exhibited an improved ability to generate cAMP, both basally in the absence of agonist and with agonist stimulation, whereas basal and maximal agonist-stimulated cAMP activity was reduced for the F282N mutant. Interestingly, the Phe^{282} mutants displayed increased sensitivity to MTSEA-mediated inhibition of radioligand binding, with an order of sensitivity (F282L > F282A > F282G = F282N) directly related to their degree of constitutive activity. This finding mimics that observed for the α_{1B}-AR Phe^{303} mutants and suggests (i) that this TMVI Phe is highly conserved in the α_{1B}- and β_2-AR structures, as well as those of other members of the biogenic amine class of GPCRs, because it plays a critical structural and functional role in the receptor−G protein activation process and (ii) that the conformational changes induced by the Phe^{282} mutants, like those for the α_{1B}-AR Phe^{303} mutants, result in one or more native TM-embedded cysteines moving into the water-accessible ligand-binding pocket. Additional substitution of endogenous cysteines, one at a time, on the Phe^{282} mutant background revealed that Cys^{285} in TMVI was entirely responsible for the MTSEA sensitivity of F282A, whereas sensitivity of F282L involved both Cys^{285} in TMVI and Cys^{327} in TMVII.

On the basis of a model of the β_2-AR that we constructed using the high-resolution X-ray structure of rhodopsin as a template, and as noted previously by Baldwin et al. (*25*), Cys^{285} points toward TMVII and is located in a boundary zone between the lipid bilayer and the water-accessible ligand-binding pocket. Given this orientation of Cys^{285}, its acquired MTSEA sensitivity in the F282A and F282L mutants likely reflects a conformational rearrangement of TMVI (rotation and/or tilting), resulting in movement of Cys^{285} into the water-accessible ligand-binding pocket. The alternate possibility that Cys^{285} becomes water-accessible because of movement of TMVII away from TMVI cannot be definitely excluded but is unlikely. Thus, in this circumstance, Cys^{285} would remain in a position in which its side chain is not directed toward the ligand-binding pocket, and in contrast to what was observed, MTSEA derivatization would not inhibit radioligand binding.

Acquired MTSEA sensitivity of Cys^{285} has also been reported for other constitutively activating mutations of the

Table 2: Ligand Binding Profiles of Phe^{282} Mutant β_2-ARs[a]

	[(−)-isoproterenol] (nM)			
construct	$K_{i,high}$	$K_{i,low}$	[(±)-CGP12177] (nM)	[[^{125}I]CYP] (pM)
F282A/C285A	2.11 ± 0.11 (0.79 ± 0.09)	34.3 ± 5.6	2.39 ± 1.1	144 ± 7
F282A/C327A	1.82 ± 0.07 (0.87 ± 0.04)	51 ± 12	1.59 ± 0.92	156 ± 48
F282L/C285A	1.37 ± 0.49* (0.83 ± 0.04)	24 ± 2.6*	1.62 ± 0.98	197 ± 52
F282L/C327A	0.45 ± 0.07* (0.79 ± 0.04)	23.2 ± 7.2*	3.93 ± 0.89	200 ± 56
F282L/C285A/C327A	1.21 ± 0.15 (0.62 ± 0.06)	144 ± 12	2.46 ± 0.79	166 ± 70
C285A		147 ± 28	2.67 ± 0.45	147 ± 58
C327A		185 ± 52	2.78 ± 1.21	160 ± 40
C285A/C327A		97 ± 22	3.89 ± 0.99	169 ± 27

[a] Using membranes prepared from transfected COS-1 cells, the binding affinities (K_i) of (−)-isoproterenol, in the presence and absence of GMP-PNP (100 μM), as well as (±)-CGP12177 were determined from [^{125}I]CYP competition binding studies. The affinity of [^{125}I]CYP (K_D) was determined by saturation binding as described in Experimental Procedures. Data are presented as means ± one standard error of at least three independent experiments, each performed in duplicate. Values in parentheses are the fraction of high-affinity binding sites. Asterisks indicate differences ($p < 0.05$) vs the respective F282A/C285A or F282A/C327A values.

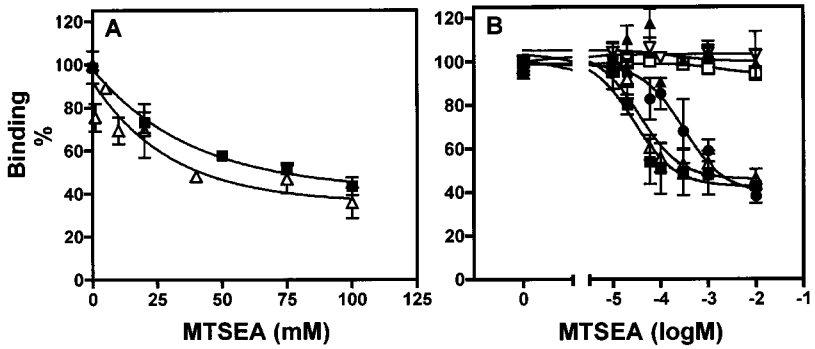

FIGURE 7: MTSEA inhibition curves from F282A to F282L/C327A, and effects of MTSEA on [^{125}I]CYP binding to wild-type and mutant β_2-ARs. (A) The MTSEA inhibition curve for F282A taken from Figure 6 was superimposed on that for F282L/C327A taken from Figure 5B. (B) COS-1 cells expressing the wild-type β_2-AR (□) or the mutants F282A (▲), F282L (▽), F290C (■), F290C/F282A (△), and F290C/F282L (●) were treated with MTSEA for 2 min. Specific [^{125}I]CYP binding was then assessed.

β_2-AR, including mutations of Asp^{130} in TMIII (*16*) and of residues at the TMVI−cytoplasmic boundary, including Glu^{268} (*17*, *26*). Importantly, movement of Cys^{285} has also been demonstrated by fluorescence spectroscopy with agonist-induced conformational changes of the β_2-AR (*4*), suggesting that this movement is intrinsic to the normal activation process.

Involvement of Cys^{327} in F282L-induced constitutive activation is somewhat surprising, since fluorescence spectroscopic evaluation of agonist-induced structural changes of the β_2-AR did not detect such movement (*4*). However, the ability of this approach to detect helical movements is critically dependent on the successful derivatization of all cysteines in question with the fluorescent probe. Given, as indicated in our model, that Cys^{327} is directed toward TMI, it is questionable if it is accessible in the absence of receptor activation. Thus, these studies do not necessarily exclude the possible involvement of TMVII in β_2-AR activation. In fact, electron paramagnetic resonance (EPR) spectroscopy studies of rhodopsin indicate that TMVII undergoes a conformational change in response to photoactivation (*27*). Moreover, Tyr^{326}, a residue adjacent to Cys^{327} and a constituent of the highly conserved NPXXY motif of GPCRs, has been shown to be involved in receptor activation and regulation (*28*, *29*). More recently, an Asn (Asn^{674}) at the cytoplasmic end of TMVII has also been implicated in the activation of the TSH receptor (*6*). Thus, conformational changes of TMVII may indeed be involved in GPCR activation.

To more fully evaluate the Phe^{282} mutant-induced TM movements, we used an engineered cysteine as a conformational sensor. In these studies, an endogenous residue, Phe^{290}, located in the upper segment of TMVI and facing the ligand-binding pocket, was substituted with a cysteine residue, on both the wild-type and Phe^{282} mutant background. Resulting mutations were then evaluated for MTSEA sensitivity. These studies showed that the F282A and F282L mutations induced different conformational changes in TMVI, with the latter causing rearrangement of not only the lower but also the upper segments of this helix. These results are consistent with our findings in the α_{1B}-AR that TMVI helical movements induced by various Phe^{303} mutants are different as well (*18*). The differential movements of the lower and upper segments of TMVI induced by F282A and F282L mutations are likely to be functionally important, since movement of this helix has been critically implicated in photoactivation of rhodopsin (*2*) and agonist activation of the β_2-AR (*4*).

TMVI of the β_2-AR contains a proline residue (Pro^{288}), which is conserved in rhodopsin-like receptors, as well as most members of the GPCR superfamily (*1*). The crystal structure of rhodopsin shows that this proline, located approximately in the middle of the helix, induces a kink (*22*). Our recent analysis of all high-resolution structures of polytopic membrane proteins, including that for rhodopsin, revealed that noncanonical elements, such as proline-induced kinks, are determined by the four to six residues immediately N-terminal to the perturbing proline (*30*). Alignment of the rhodopsin, α_{1B}-AR, and β_2-AR residues N-terminal to this

proline reveals remarkable primary structure conservation (FLICWLP, FILCWLP, and FTLCWLP, respectively), indicating that a kink is likely present in TMVI of these receptors and other members of the biogenic amine class of GPCRs. Moreover, substitution of this proline with alanine, which is likely to disrupt the kink, results in constitutive activation of both the yeast α-factor receptor (*31*) and the α_{1B}-AR (unpublished data), suggesting that the presence of the kink in TMVI is critical for receptor activation.

On the basis of the finding that, with activation, TMVI in rhodopsin moves as a rigid body (*2*), as well as site-selective fluorescent labeling studies of the β_2-AR that are entirely consistent with TMVI moving as a rigid body (*32*), we propose that the proline in TMVI, rather than adding flexibility, as suggested by Ballestros and Weinstein (*23*) and Gether et al. (*4*), simply kinks and rigidifies the helix. The rigid, kinked helical rod then may act as a pivot for amplification of the conformational changes associated with agonist binding, and for productive propagation of the agonist signal to the G protein-interacting TMVI−cytoplasmic receptor interface. By virtue of its rigid kinked angle, TMVI provides a larger sweep at its ends than that possible with a straight or flexible helix. For this simple mechanical reason alone, we think it probable that the proline-induced kink in the middle of this helix has evolved, and has been maintained through evolution, as a transmitter and an amplifier of the rotational momentum about the kink. Nevertheless, this hypothesis remains to be substantiated by further experiments.

Given the fact that Phe^{282} is highly conserved in GPCRs, this residue may be involved in an activation process that is common to many receptors. Indeed, like β_2-AR Phe^{282} mutants, various substitutions of the Phe^{282} equivalent in the muscarinic (M_5) receptor (Phe^{451}) result in mutants with altered signaling activity (*5*). Studies of rhodopsin also suggest that the residue equivalent to Phe^{282} in the β_2-AR, i.e., Phe^{261}, functionally interacts with Gly^{121} in TMIII, and that this interaction is involved in rhodopsin activation (*33*). Interestingly, in a recent report by Baranski et al. (*7*), using random saturation mutagenesis of the C5a receptor, the Phe^{282} equivalent was identified as one of the residues that comprise the core switch domain for G protein activation. Moreover, mutation of this residue (Phe^{347}) to alanine in the cholecystokinin B receptor (*34*) has been shown to inactivate the receptor. Conceivably, therefore, agonist binding or mutations that disrupt the TMIII−TMVI interaction result in receptor activation. In support of this notion, it has been shown recently that a conserved TMIII Arg (Arg^{131}) in the β_2-AR forms an ionic bond with Asp^{130} and Glu^{268} at the cytoplasmic end of TMVI. That this interaction serves to constrain the receptor in an inactive state was evident from charge-neutralizing mutations of either Asp^{130} or Glu^{268}, which resulted in constitutive receptor activation.

Why the F282A and F282L mutations induce different conformational movements is unclear but may be related to the different side chain characteristics of the substituents. For example, although both mutations may disrupt interhelical interactions between TMIII and TMVI, unlike the Leu side chain of the F282L mutation, that of the Ala substitution, which is short and lacks hydrophobicity, may not allow new interhelical interactions required to stabilize the active conformation.

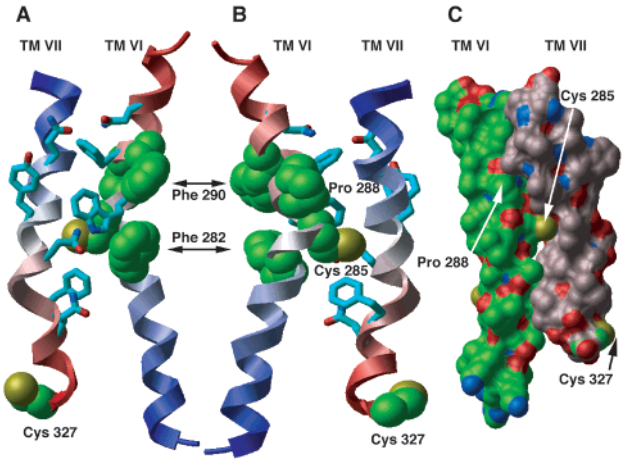

FIGURE 8: Three-dimensional model of the β_2-AR TMVI−TMVII interface. (A) Ribbon diagram of TMVI and VII helices with selected residues highlighted in space-filling CPK representation or as sticks. Transmembrane helical segments are color-coded from blue to red from the N-terminus to the C-terminus. Note the prominent kinks visible in both helices. Phe^{282}, Phe^{290}, Pro^{288}, Cys^{285}, and Cys^{327} are shown in space-filling representations with carbons in green. Also shown as light blue sticks are residues Trp^{286}, Phe^{289}, Asn^{292}, Asn^{312}, Tyr^{316}, Phe^{321}, and Asn^{322}. (B) Same as panel A but with the two helices rotated approximately 180°. (C) Surface representation of TMVI and -VII helices showing the tightly packed interhelical interface. Selected residues are labeled. Carbon surfaces in TMVI are green; those in TMVII are pink.

With respect to the potential involvement of TMVII in the conformational movements associated with receptor activation, evidenced by our finding of de novo water accessibility of Cys^{327} with the activated F282L mutant, our β_2-AR model indicates that a plausible mechanism for the propagation of activation-induced movements over a distance of ~28 Å from the ligand-interacting Phe^{290} residue in TMVI to Cys^{327} in TMVII is by mechanical momentum transfer through long, rigid structures such as (straight or kinked) helices. This proposal seems to be well-supported by the exceptional nature of the TMVI−TMVII helical interface (Figure 8). There, bulky aromatic side chains interacting in typical herringbone arrangements (*35*) are mixed with strongly dipolar amide side chains (Asn^{293,312,318,322}). The charged Asp^{113} provided by TM helix III packs against the upper part of TMVII. It has been known that buried amide side chains, or even charged ones, may interact effectively with aromatic π systems of Phe, Tyr, and Trp residues inside proteins achieving thermodynamically stable dipolar/aromatic clusters (*35*). Any "local" changes to these clusters, such as ligand-induced residue rearrangements in receptor binding sites, e.g., that for Phe^{290}, are likely to affect stability of whole clusters, possibly inducing large-scale movements of side chains propagating along the length of the transmembrane helices. Interestingly, recent studies by Govaerts et al. indicate that an Asn (Asn^{674}) at the cytoplasmic end of TMVII in the TSH receptor interacts with Asp^{633} in TMVI, a residue equivalent to the β_2-AR Phe^{282}, and such interaction is important to constrain the receptor in the inactive state (*6*). Thus, it is likely that relative movements of both TMVI and VII are critically involved in receptor activation.

It should be noted that although both the β_2-AR and α_{1B}-AR Phe (positions 282 and 303, respectively) mutants have altered functional activity, their signaling and agonist binding profiles are not entirely the same. Thus, all β_2-AR Phe^{282}

mutants, except F282N, exhibit increased basal activity and maximal (−)-isoproterenol-stimulated cAMP accumulation; on the other hand, the signaling activity of the α_{1B}-AR F303G and F303N mutants is abolished, both basally and with agonist stimulation (*3*), and the F303A mutant displays increased basal activity but a reduced maximal agonist response (*18*). Also, the β_2-AR F282N mutant, although showing reduced signaling activity, unlike its α_{1B}-AR counterpart (*3*), does not exhibit dominant negative activity when coexpressed with the wild-type β_2-AR (data not shown). Finally, all Phe^{282} mutants, except F282N, display increased agonist binding affinity, which, in part, is due to G protein precoupling, since treatment with GMP-PNP significantly reduced their affinity. This contrasts with the GMP-PNP-insensitive agonist binding of the α_{1B}-AR Phe^{303} mutants (*18*). Thus, although the general role of the Phe in receptor activation is conserved, effects of its substitution on receptor function and ligand binding show subtle differences. This is not surprising, given that the sequence identity between the α_{1B}- and β_2-AR is limited. Thus, the residues interacting with this TMVI Phe in the native receptor structures are likely to vary from one receptor to another.

ACKNOWLEDGMENT

We are grateful to Drs. Siiri Iismaa and Ahsan Husain for critical reading of the manuscript.

REFERENCES

1. Gether, U. (2000) *Endocr. Rev. 21*, 90−113.
2. Farrens, D. L., Altenbach, C., Yang, K., Hubbell, W. L., and Khorana, H. G. (1996) *Science 274*, 768−770.
3. Chen, S. H., Lin, F., Xu, M., Hwa, J., and Graham, R. M. (2000) *EMBO J. 19*, 4265−4271.
4. Gether, U., Lin, S., Ghanouni, P., Ballesteros, J. A., Weinstein, H., and Kobilka, B. K. (1997) *EMBO J. 16*, 6737−6747.
5. Spalding, T. A., Burstein, E. S., Henderson, S. C., Ducote, K. R., and Brann, M. R. (1998) *J. Biol. Chem. 273*, 21563−21568.
6. Govaerts, C., Lefort, A., Costagliola, S., Wodak, S. J., Ballesteros, J. A., Van Sande, J., Pardo, L., and Vassart, G. (2001) *J. Biol. Chem. 276*, 22991−22999.
7. Baranski, T. J., Herzmark, P., Lichtarge, O., Gerber, B. O., Trueheart, J., Meng, E. C., Iiri, T., Sheikh, S. P., and Bourne, H. R. (1999) *J. Biol. Chem. 274*, 15757−15765.
8. Lefkowitz, R. J., Cotecchia, S., Samama, P., and Costa, T. (1993) *Trends Pharmacol. Sci. 14*, 303−307.
9. Pauwels, P. J., and Wurch, T. (1998) *Mol. Neurobiol. 17*, 109−135.
10. Robinson, P. R., Cohen, G. B., Zhukovsky, E. A., and Oprian, D. D. (1992) *Neuron 9*, 719−725.
11. Porter, J. E., Hwa, J., and Perez, D. M. (1996) *J. Biol. Chem. 271*, 28318−28323.
12. Porter, J. E., and Perez, D. M. (1999) *J. Biol. Chem. 274*, 34535−34538.
13. Cohen, G. B., Yang, T., Robinson, P. R., and Oprian, D. D. (1993) *Biochemistry 32*, 6111−6115.
14. Acharya, S., and Karnik, S. S. (1996) *J. Biol. Chem. 271*, 25406−25411.
15. Scheer, A., Fanelli, F., Costa, T., De Benedetti, P. G., and Cotecchia, S. (1997) *Proc. Natl. Acad. Sci. U.S.A. 94*, 808−813.
16. Rasmussen, S. G. F., Jensen, A. D., Liapakis, G., Ghanouni, P., Javitch, J. A., and Gether, U. (1999) *Mol. Pharmacol. 56*, 175−184.
17. Javitch, J. A., Fu, D. Y., Liapakis, G., and Chen, J. Y. (1997) *J. Biol. Chem. 272*, 18546−18549.
18. Chen, S., Lin, F., Xu, M., and Graham, R. M. (2002) *Biochemistry 41*, 588−596.
19. Noda, K., Saad, Y., Graham, R. M., and Karnik, S. S. (1994) *J. Biol. Chem. 269*, 6743−6752.
20. Chen, S., Xu, M., Lin, F., Lee, D., Riek, P., and Graham, R. M. (1999) *J. Biol. Chem. 274*, 16320−16330.
21. Bradford, M. M. (1976) *Anal. Biochem. 72*, 248−254.
22. Palczewski, K., Kumasaka, T., Hori, T., Behnke, C. A., Motoshima, H., Fox, B. A., Le Trong, I., Teller, D. C., Okada, T., Stenkamp, R. E., Yamamoto, M., and Miyano, M. (2000) *Science 289*, 739−745.
23. Ballesteros, J. A., and Weinstein, H. (1995) *Methods Neurosci. 25*, 366−428.
24. Strader, C. D., Sigal, I. S., and Dixon, R. A. (1989) *FASEB J. 3*, 1825−1832.
25. Baldwin, J. M., Schertler, G. F., and Unger, V. M. (1997) *J. Mol. Biol. 272*, 144−164.
26. Ballesteros, J. A., Jensen, A. D., Liapakis, G., Rasmussen, S. G., Shi, L., Gether, U., and Javitch, J. A. (2001) *J. Biol. Chem. 276*, 29171−29177.
27. Altenbach, C., Cai, K., Khorana, H. G., and Hubbell, W. L. (1999) *Biochemistry 38*, 7931−7937.
28. Gabilondo, A. M., Krasel, C., and Lohse, M. J. (1996) *Eur. J. Pharmacol. 307*, 243−250.
29. Barak, L. S., Menard, L., Ferguson, S. S., Colapietro, A. M., and Caron, M. G. (1995) *Biochemistry 34*, 15407−15414.
30. Riek, R. P., Rigoutsos, I., Novotny, J., and Graham, R. M. (2001) *J. Mol. Biol. 306*, 349−362.
31. Konopka, J. B., Margarit, S. M., and Dube, P. (1996) *Proc. Natl. Acad. Sci. U.S.A. 93*, 6764−6769.
32. Jensen, A. D., Guarnieri, F., Rasmussen, S. G., Asmar, F., Ballesteros, J. A., and Gether, U. (2001) *J. Biol. Chem. 276*, 9279−9290.
33. Han, M., Lin, S. W., Minkova, M., Smith, S. O., and Sakmar, T. P. (1996) *J. Biol. Chem. 271*, 32337−32342.
34. Jagerschmidt, A., Guillaume, N., Roques, B. P., and Noble, F. (1998) *Mol. Pharmacol. 53*, 878−885.
35. Burley, S. K., and Petsko, G. A. (1985) *Science 229*, 23−28.

BI012189C